The gene *ENHANCER OF PINOID* controls cotyledon development in the *Arabidopsis* embryo

Birgit S. Treml[1], Sabine Winderl[1,*], Roman Radykewicz[1,†], Markus Herz[2], Günther Schweizer[2], Peter Hutzler[3], Erich Glawischnig[1] and Ramón A. Torres Ruiz[1,‡]

[1]Lehrstuhl für Genetik, Technische Universität München, Wissenschaftszentrum Weihenstephan, Am Hochanger 8, 85350 Freising, Germany
[2]Bayerische Landesanstalt für Landwirtschaft, Institut für Pflanzenbau und -züchtung, IPZ 1b, Am Gereuth 2, 85354 Freising, Germany
[3]Institut für Pathologie, GSF-Forschungszentrum für Umwelt und Gesundheit GmbH, 85764 Neuherberg, Germany
*Present address: ALTANA Pharma AG, Byk-Gulden-Str. 2, 78467 Konstanz, Germany
†Present address: Institut für Toxikologie, GSF–Forschungszentrum für Umwelt und Gesundheit GmbH, 85764 Neuherberg, Germany
‡Author for correspondence (e-mail: ramon.torres@wzw.tum.de)

Accepted 5 July 2005

Development 132, 4063-4074
Published by The Company of Biologists 2005
doi:10.1242/dev.01969

Summary

During *Arabidopsis* embryo development, cotyledon primordia are generated at transition stage from precursor cells that are not derived from the embryonic shoot apical meristem (SAM). To date, it is not known which genes specifically instruct these precursor cells to elaborate cotyledons, nor is the role of auxin in cotyledon development clear. In *laterne* mutants, the cotyledons are precisely deleted, yet the hypocotyl and root are unaffected. The *laterne* phenotype is caused by a combination of two mutations: one in the *PINOID* (*PID*) gene and another mutation in a novel locus designated *ENHANCER OF PINOID* (*ENP*). The expression domains of shoot apex organising genes such as *SHOOT MERISTEMLESS* (*STM*) extend along the entire apical region of *laterne* embryos. However, analysis of *pid enp stm* triple mutants shows that ectopic activity of *STM* does not appear to cause cotyledon obliteration. This is exclusively caused by *enp* in concert with *pid*. In *pinoid* embryos, reversal of polarity of the PIN1 auxin transport facilitator in the apex is only occasional, explaining irregular auxin maxima in the cotyledon tips. By contrast, polarity of PIN1:GFP is completely reversed to basal position in the epidermal layer of the *laterne* embryo. Consequently auxin, which is believed to be essential for organ formation, fails to accumulate in the apex. This strongly suggests that *ENP* specifically regulates cotyledon development through control of PIN1 polarity in concert with *PID*.

Key words: *laterne, PINOID*, *ENHANCER OF PINOID*, Embryo, *Arabidopsis*, Pattern formation, Auxin, PIN1, Organogenesis, Cotyledons

Introduction

Cotyledons are specialized storage organs for lipids, proteins and starch, and are indispensable for the survival of the young seedling. In *Arabidopsis*, they are initiated towards the end of the globular stage. As a consequence, the radial symmetry of the globular embryo transitions to the bilateral symmetry of the heart stage embryo (for a review, see Torres Ruiz, 2004). Comparative and evolutionary considerations, as well as genetic analysis (including *leafy cotyledon* and *extra cotyledon* mutants) suggest that cotyledons and adult leaves are homologous structures (Meinke, 1992; Lotan et al., 1998; Stone et al., 2001; Convay and Poethig, 1997; Strasburger, 2002; Kaplan and Cooke, 1997; Tsukaja, 2002). The relationship between cotyledons and true leaves led to the conclusion that cotyledons are generated by an embryonic SAM embracing the entire apex of the globular embryo (Kaplan, 1969; Kaplan and Cooke, 1997). However, mutations in the *Arabidopsis STM* (and other genes) affect the SAM, but leave the cotyledons largely unaffected (Long et al., 1996; Mayer et al., 1998; Moussian et al., 1998; Lynn et al., 1999). This suggests that cotyledons, unlike true leaves, arise independently from the (embryonic) SAM. Accordingly separation of SAM and the cotyledon anlagen is established during the early globular stage and *STM* is expressed in between the cotyledon anlagen (Long et al., 1996). Conversely, the region where cotyledon primordia arise is marked by the expression of genes such as *AINTEGUMENTA* (*ANT*), *FILAMENTOUS FLOWER* (*FIL*) and *ASYMMETRIC LEAVES 1* and *ASYMMETRIC LEAVES 2* (*AS1*, *AS2*) (Elliott et al., 1996; Klucher et al., 1996; Siegfried et al., 1999; Byrne et al., 2000, Iwakawa et al., 2002). Three partially redundant *CUP-SHAPED COTYLEDON1-CUP-SHAPED COTYLEDON3* genes (*CUC1-CUC3)* specify boundary regions to separate cotyledons from each other. Their expression patterns initially overlap with *STM* (Aida et al., 1997; Aida et al., 1999; Vroemen et al., 2003).

Aerial organs, e.g. leaves, are believed to be induced when local (initially stochastic) concentrations of auxin form. This hormone is transported in the epidermal layer towards the incipient organ primordium to give rise to groups of cells that accumulate high concentrations of auxin at its tip, which itself might produce auxin (Benkova et al., 2003; Ljung et al., 2001).

From these sites, auxin is transported downwards through the vascular elements in direction to the root. In the aerial organs, the directed auxin transport is promoted by the PIN1 transport facilitator, which is located at apical sites in the epidermis and at basal sites in the stele (Gälweiler et al., 1998; Benkova et al., 2003). Studies, including microapplication experiments, suggest that a developing leaf depletes local auxin pools and determines the spatial arrangement of the next maximum (phyllotaxis) (Reinhardt et al., 2003). Whether auxin maxima are required for the initiation and/or maintenance of cotyledon primordia remained to be determined.

The establishment of a comprehensive model for the pattern formation in the *Arabidopsis* embryo has been hampered by the absence of cotyledon-specific genes (Berleth and Chatfield, 2002). Analyses of several *Arabidopsis* mutants found in embryonic pattern screens (e.g. Mayer et al., 1991; Scheres et al., 1995) showed that the generation of cotyledons is notoriously sensitive to disturbances in diverse biological processes. For example, the reduction to complete elimination of cotyledons occurs in *gurke* and *pepino/pasticcino2*, which are thought to regulate cell proliferation (Torres et al., 1996a; Haberer et al., 2002; Baud et al., 2004). Mutations in a number of genes related to auxin transport or sensing give rise to seedlings with fused cotyledons or altered cotyledon numbers (Okada et al., 1991; Berleth and Jürgens, 1993; Mayer et al., 1993; Bennett et al., 1995; Geldner et al., 2004; Friml et al., 2004). A deletion of the cotyledons occurs especially when two or more such mutants are combined, as observed in quadruple mutants of *pin-formed1*, *pin-formed3*, *pin-formed4* and *pin-formed7* (Friml et al., 2003). Recently, Furutani et al. (Furutani et al., 2004) have shown that the double mutant *pin1 pid* results in ~50% cotyledonless seedlings. In contrast to the above mentioned genes, which affect a number of organs (or, which have pleiotropic effects), *laterne* mutants are characterized by a specific and precise deletion of the cotyledons.

The *laterne* phenotype is caused by a combination of two mutations, one in *PINOID* and the other in an unknown gene designated *ENHANCER OF PINOID,* and is characterized by a specific and precise deletion of the cotyledons. The detection of *ENP* uncovers a cotyledon specific genetic programme and provides a new gateway for understanding cotyledon development and the impact of auxin in the embryo apex**.**

Materials and methods

Plant strains and growth conditions

The L*er* ecotype was used as wild-type reference. The *laterne* segregating line originates from an EMS mutagenesis in the L*er* background and has been isogenized by selfing repeatedly (Torres et al., 1996b). The induced alleles are designated *enp* and *pid*-15, which has a G to A transition changing amino acid 380 from G to E. Additionally, the following *pinoid* alleles were used (Bennett et al., 1995; Christensen et al., 2000): *pid-2* (*Ler* background; G to R change at amino acid 380; intermediate); *pid-8* (WS background; P to Q change at amino acid 300; weak) and *pid-9* (Col background; deletion from 526-548 leading to a truncation after R175; strong). The *stm-5* mutation is a G to A transition (first nucleotide) of the 5′-splice site in the third intron of *STM* and leads to a strong phenotype (T. Laux, personal communication). Plants were grown as previously described (Haberer et al., 2002) except that some batches were grown in a 12 hours light/12 hours dark cycle.

Genetic analyses and mapping

The homozygous *enp/enp* line originated from the selfing of a line carrying one *pid-15* and at least one *enp* allele. As the *enp* phenotype is subtle, the presence of *enp/enp*, in all genotype combinations generated by conventional crosses, was confirmed by crossing with *pid*-alleles and checking following generations for the occurrence of *laterne* seeds (see Fig. S1 and Table S1 in the supplementary material). Segregation analysis showed that *enp* exhibits full penetrance (see Table S2 in the supplementary material). Generation of homozygous *pid-15 enp stm-5* mutants was performed by generating *pid-15 enp stm-5/+ enp* + plants. These segregated only three classes of seedling phenotypes: wild type, *stm* and *laterne*. This progeny was then subjected to analysis by pyrosequencing, which scored for homo- or heterozygosity in both the *STM* and the *PINOID* gene. We analysed 102 wild-type, 62 *laterne* and 41 *stm* seedlings or adult plants (the numbers do not represent segregation as seedlings were processed as they grew). Simultaneous homozygosity for *pid-15* and *stm-5* was detected only in the fraction of *laterne* seedlings. In addition, *pid-15* + *stm-5/pid-15* + + plants were generated, which produce seedlings with either *pinoid* or *stm-5* phenotypes (19/67 with *stm* phenotype). Mapping of the *ENP* locus was carried out with CAPS and the complete set of SSLP markers as described (Lukowitz et al., 2000; Haberer et al., 2002) by using F2 *laterne* plants (genotype *pid-15 enp/pid-15 enp*, but see below). These had been generated by crosses of *pid-15 enp/+ enp* with the polymorphic ecotypes Col and Nd (Erschadi et al., 2000). Primers were: 5′-GGACGTAGAA-TCTGAGAGCTC-3′ and 5′-GGTCATCCGTTCCCAGGTAAAG-3′ for G4539 (CAPS marker); and 5′-AATTTGGAGATTAGCTGGAAT-3′ and 5′-CCATGTTGATGATAAGCACAA-3′ for ciw7 (SSLP marker). The formula $p=1-\sqrt{(1-x)}$ was used for linkage calculation (x=ratio of recombinant plants; p=calculated recombination frequency) correcting for p-values greater than 10% using the Kosambi function. The linkage found was ~18.9 cM (76/233 recombinants for G4539) and ~9.9 cM (44/233 recombinants for ciw7). In rare cases, *pid* homozygous plants produce leaky *laterne* seeds (see Table S3 in the supplementary material). However, the resulting differences to the genetic distance values given above are negligible.

Microscopy

Semi-thin sections and whole mount analysis of embryos and seedlings were carried out as previously described (Haberer et al., 2002). Photographs were taken using a ZEISS Axiophot 1 microscope with 35 mm in system cameras (MC80 DX) or an adapted Kodak DCS760 system (with Digital Nikon camera F5SLR) with corresponding software (Kodak Photo Desk DCS). Epifluorescence microscopy on the same Axiophot used a HBO50 UV/Light-source with an AHF filter system F41-017. Laser-scanning microscopy was performed on a Zeiss LSM 510 META with an 488 nm Argon-Laser. The promotor GFP fusion *DR5rev::GFP* and the translational fusion PIN1:GFP have been previously described (Benkova et al., 2003; Friml et al., 2003).

Auxin transport measurements

Polar auxin transport was determined essentially as described (Okada et al., 1991). Stem segments (2.5 cm; 0.5 to 3.0 cm from the base) were inverted and placed in a solution of ^{14}C-IAA (0.1 μCi/ml) in 5 mM MES (pH 5.7)/1% sucrose. After 24 hours the stem segments were dried on filter paper for 5 minutes and then analyzed after autoradiography for a minimum of 10 days using a Storm 860 phosphoimager. For each stem segment ^{14}C-IAA was quantified in the basal 4 mm (see Table S4 in the supplementary material).

RT-PCR and (Pyro-)sequencing

RNA isolation, reverse transcription and PCR were performed according to the supplier's instructions using a NucleoSpin-RNA Plant kit (Macherey-Nagel) and a TaqMan kit (Applied Biosystems, Roche), respectively (Fig. S2).

PCR bands, generated from *pid-15* and *stm-5* DNA as template, were sequenced using the BigDye® Terminator v1.1 Cycle Sequencing Kit on an ABI prism sequencer according to the manufacturer's instructions. The data were analysed with the Lasergene Seq Man™ II programme by DNA STAR.

Pyrosequencing reactions were performed by the PSQ MA 96 system (Biotage, Sweden) using ThermoStart DNA Polymerase (ABGene, Germany) according to the manufacturer's protocols. Primers, designed using the Pyrosequencing Assay Design Software version 1.0.6., were as follows: 5′-CATGCGCGGAATTTGATTT-3′; Biotin-5′-CTTGACGACGGAAGAAGGAATC-3′; and 5′-GATCC-GACTAAAAGACTTG-3′ for *PID/pid-15*; 5′-CCCTAAAGAAGC-TCGTCAACA-3′; Biotin-5′-AGTATGGATGCAAAAATCACAAA-3′ and 5′-TGGCCTTACCCTTCG-3′ for *STM/stm-5*.

In situ hybridisation analyses

In situ hybridization was essentially performed as described (Schoof et al., 2000). Sense probes were used as controls and wild-type expression patterns for all probes were confirmed. Hybridisations were performed at 50°C with the *CUC2* probe and the *WUS* probe and at 55°C with the *ANT* and the *STM* probe, respectively. We evaluated 69 embryos (10/69 *laterne*) with *CUC2,* 96 embryos (23/96 *laterne*) with *WUS*, 40 embryos (11/40 *laterne*) with *ANT* and 64 embryos (12/64 *laterne*) with *STM* (numbers are not representative for segregation; embryos were selected depending on quality and orientation). Templates for transcription were kindly provided by K. Barton (merih5-clone with *STM* gene) (Long et al., 1996), D. Smyth (*ANT* gene) (Elliott et al., 1996), M. Aida (*CUC2* gene) (Aida et al., 1999) and T. Laux (*WUS* gene) (Mayer et al., 1998).

Results

The mutant *laterne* lacks cotyledons and develops an altered shoot apex topology

The *laterne* mutant exhibits a precise deletion of the cotyledons (Fig. 1). Cells constituting the embryonic root meristem and root cap, respectively, or the different tissues establishing the hypocotyl are essentially wild-type in their arrangement and shape (Fig. 2). The region above the cotyledons including the SAM (i.e. epicotyl) displays one additional alteration from wild type, in that the apical tip forms an indentation instead of being elevated (for convenience called apical cavity; Fig. 2A-M). Cells of the L1 to L3 layers in this area are small and densely stained (Fig. 2A-L). They retain meristematic capability leading to primordia for true leaves, which can be distinguished from cotyledons by the appearance of trichomes (Fig. 2A-G,N-Q).

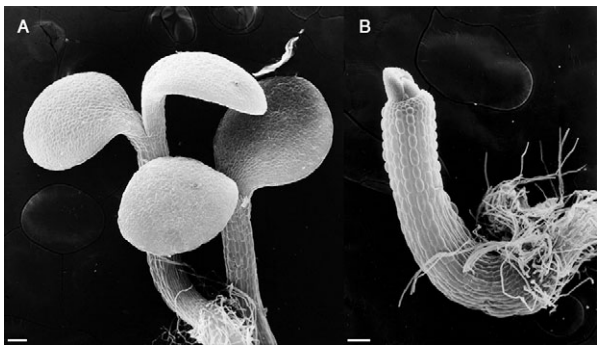

Fig. 1. Comparison of wild-type and *laterne* seedlings. (A) Wild-type and (B) *laterne* seedling under scanning electron microscopy. Scale bars: 100 μm.

The number and position of these primordia appear random in *laterne*, ranging from one for a single leaf, sometimes developing a fused cup-shaped appearance (not shown), to the simultaneous development of multiple leaf primordia (Fig. 2N). The cup-like leaves originate from ring-shaped primordia as evidenced by in situ hybridisation analyses (see below). In contrast to *cuc1,2* double mutants (Aida et al., 1997), *laterne* mutants do not suppress the SAM formation.

The earliest morphological deviation of *laterne* from wild type is visible at early heart stage when, normally, cotyledon primordia bulge out (compare Fig. 3A with 3F). It is probable this mutant does not develop cotyledon anlagen. Nevertheless, *laterne* embryos continue with an apparently wild-type development of hypocotyl and root. Consequently, longitudinal sections of *laterne* embryos do not differ from median sections of wild-type embryos (Fig. 3). At embryo maturity, *laterne* mutants can readily be recognised by the cylindrical appearance of their seed, which is a scorable phenotype (see Fig. S1 in the supplementary material).

The *laterne* phenotype is caused by two mutations: *pinoid* and *enhancer of pinoid*

ENHANCER OF PINOID was uncovered by outcrossing *laterne* to L*er* and other ecotypes. The resulting progeny lines segregated

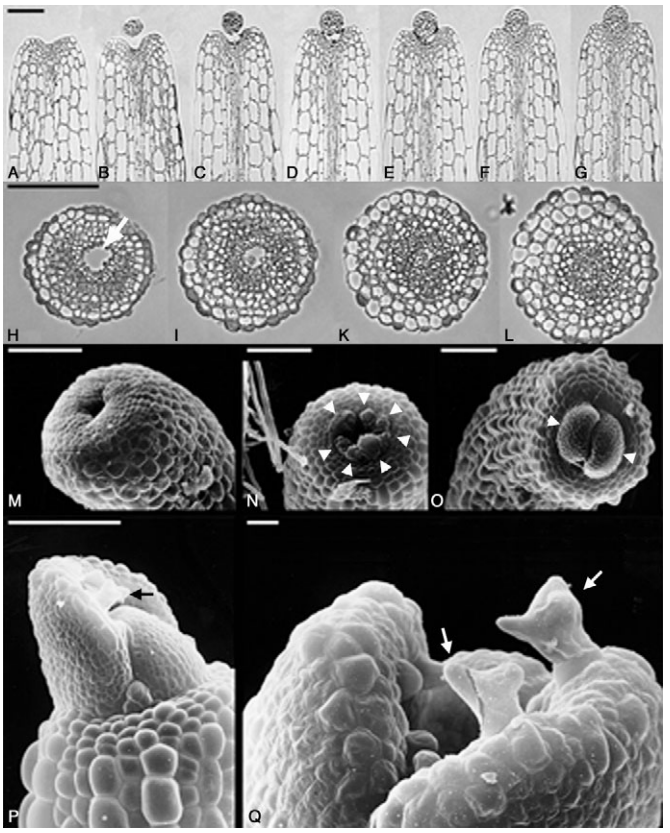

Fig. 2. Semi-thin sections and SEM of *laterne* seedlings. (A-G) Longitudinal sections of *laterne* with emerging primary leaf primordium. (H-L) Cross-sections of *laterne* showing the apical cavity (arrow) harbouring small densely stained cells. (M-Q) SEM of different *laterne* seedlings. Generation of variable numbers of leaf primordia (arrowheads; N,O) with young trichomes (P,Q; black and white arrows, respectively). Scale bars: 100 μm in A-P; 10 μm in Q.

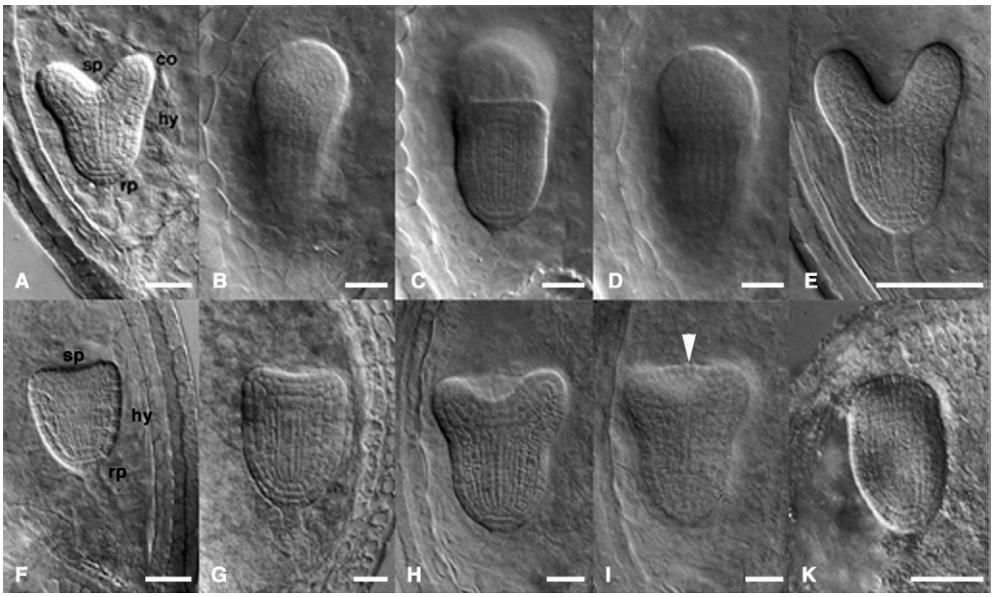

Fig. 3. *laterne* embryo development. (A) Wild-type early heart stage (frontal view). (B-D) Wild-type heart stage series (lateral view). (C) Median optical section comparable to *laterne* (*pid-15 enp*) embryo in G. (E) Wild-type late heart stage. (F,G,K) *laterne* early, mid and late heart stage (K, lateral view). (H,I) A *pid-15* embryo with three cotyledons (arrowhead points to third cotyledon). sp, shoot pole; co, cotyledon primordia; hy, hypocotyl; rp, root pole. Nomarski optics. Scale bars: 25 μm.

either wild-type, *laterne* and/or a second seedling phenotype with three cotyledons. These seedlings elaborated pin-like stems with abnormal flowers (Fig. 4), reminiscent of the mutants *pinformed1* (*pin1*) and *pinoid* (*pid*) (Okada et al., 1991; Bennett et al., 1995). Complementation analyses with *pin1* and *pid* indicated that the observed mutation represents a new allele of *pinoid*, (designated *pid-15*) harbouring a point mutation changing G to E at position 380, a conserved amino acid residue of the *PINOID* kinase. As outcrossing did not reveal an obvious third phenotype, we suspected that a second gene behaving as a modifier, induced the *laterne* phenotype in concert with *pinoid*. We termed this modifier *enhancer of pinoid* (*enp*), as it strengthens the *pinoid* seedling phenotype such that cotyledons are completely missing instead of being supernumerary. Outcrossing led to the isolation of a line that exhibits the genotype + *enp*/+ *enp* ('+' stands for wild-type allele of *PINOID*). Seeing that *enp* mutants have an almost negligible phenotype (see below), the presence of *enp* was always scored in *pid* background. Accordingly, *enp*/*ENP* was mapped by analysing *laterne* plants (see Materials and methods). *ENP* maps to the lower arm of chromosome four, 9.9 cM south of ciw7. As expected *laterne* plants also show linkage to second chromosome markers due to the mutation in *PINOID* (not shown).

Several lines were constructed in order to examine different

Fig. 4. Adult and flower phenotypes of different *enp pid* combinations. Genotypes are indicated for adult plants (upper row) and their corresponding flowers or pin-ends (middle and bottom row). The pin-ends in the third row belong to plants of the two adjacent genotypes, as indicated by white arrows. The black arrow indicates a flowerless blind ending stem of *pid*-9 +/*pid*-9 +. The black arrowhead indicates flower structures on a stem of a *pid*-9 *enp*/*pid*-9 *enp* plant. White arrowheads refer to sepal fusions. Scale bars: 1 cm (upper row); 1 mm (middle and lower rows).

combinations of *PID*/*pid* and *ENP*/*enp* (Fig. 4). Analysis of plants with the genotypes *pid-x enp*/+ *enp* or *pid-x* +/+ *enp* (*pid-x enp*/+ +; *x* represents any *pid* allele) revealed that *enp* behaves as a recessive, fully penetrant, mendelian mutation in exerting its effect in combination with *pinoid* with respect to cotyledon formation (see Tables S1 and S2 in the supplementary material). The *enp* mutation is not endogenous to L*er* ecoptype but is an EMS-induced mutation.

We tested, with respect to cotyledon formation, whether *enp* could act as enhancer of loci other than *pid*, notably *pin1*, *cuc1* and *cuc2*, as these mutants exhibit cotyledon defects partly similar to those seen in *pinoid* mutants (Okada et al., 1991; Bennett et al., 1995; Aida et al., 1997). In no case did we recover *laterne* seeds from F1 plants that were heterozygous for *enp* and one of these mutant loci. We conclude that during embryogenesis *enp* acts as a specific enhancer of *pid.*

ENP is required in late adult stages

Analysis of homozygous and heterozygous *enp* alone, as well as all heterozygous combinations of *enp* and different *pinoid* alleles revealed mild but significant floral defects in adult plants. Most notably fused organs and a variation in organ number were observed (Figs 4, 5). L*er* exhibits (less pronounced) divergence in organ numbers (Fig. 5). Adult *pid-15 enp* and *pid-2 enp* homozygous plants elaborate stems with blind ends. These mutants completely lack floral structures but occasionally generate terminally stigmatic tissue (not shown). This enhancement of *pinoid* floral defect by *enp*, however, depends on the genetic background, as combinations of *enp* with *pid*-8 and *pid*-9 originating from other backgrounds produce at least some, though sterile, abnormal flowers (Figs 4, 5). This notion is supported by outcrossing *pid-15 enp* (L*er* background) to Col, which led to (rare) *laterne* plants with few floral structures (not shown). Considering different allele and background combinations, we found only two consistent effects in homozygous *enp pid* double mutants: significant reduction of sepals and sterility because of a reduction of gynoecia.

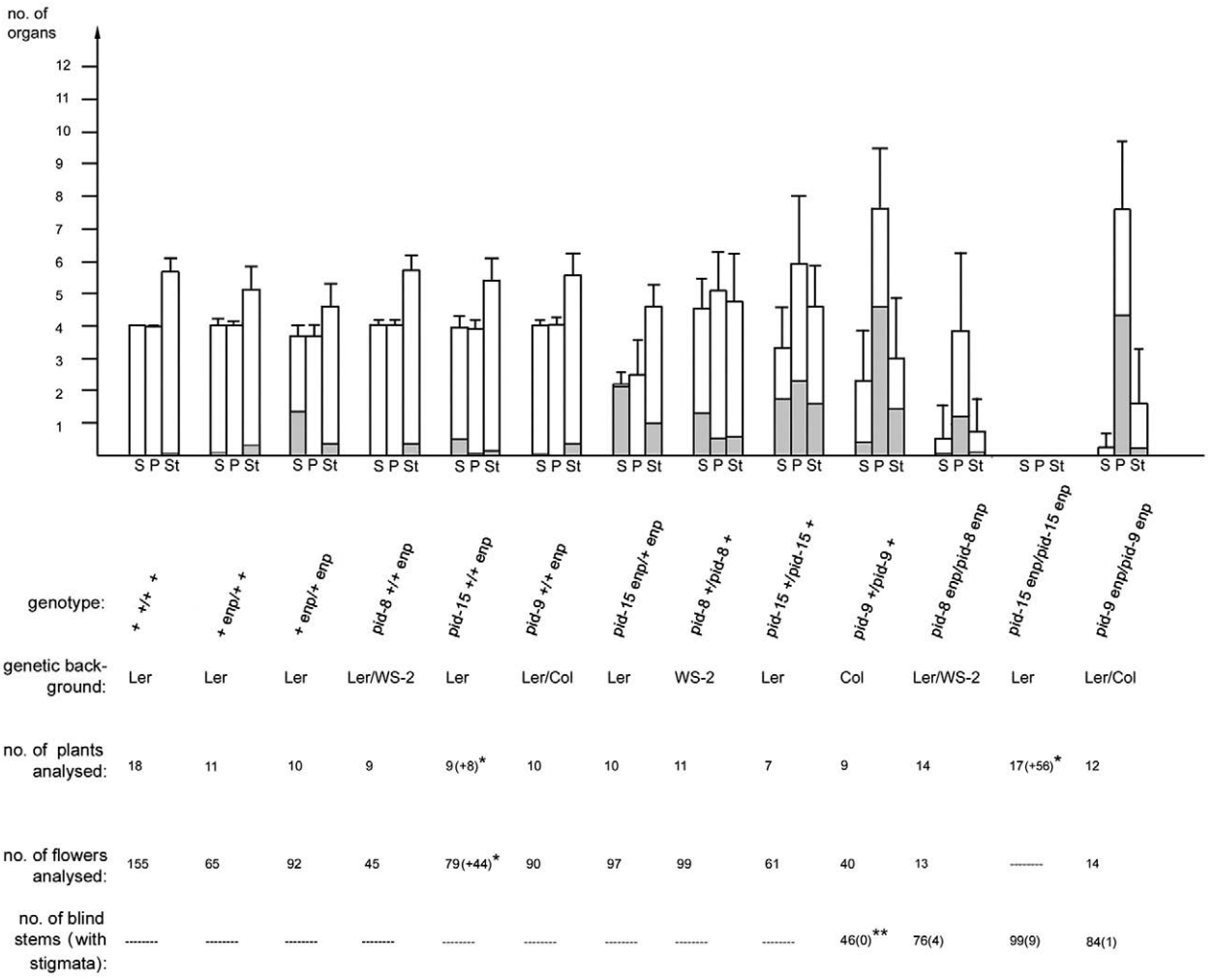

Fig. 5. Development of flower organs in *enp* and *pid* combinations. Sepals (S), petals (P) and stamens (St) were scored. Mean values and standard deviations are given. Shaded regions indicate the occurrence of organ fusion (in % of all flowers examined; e.g. 98% fusion of sepals in *pid-15 enp*/+ *enp*). The *pid* homozygous plants developed variably reproductive gynoecia, whereas *pid enp*/*pid enp* double mutants led to collapsed gynoecia or completely lacked flowers. Wild-type, + +/+ *enp*, + *enp*/+ *enp* and *pid*-x +/+ *enp* plants did not display conspicuous infertility. The *pid enp*/+ *enp* plants exhibited partial fertility, while *pid*-x *enp*/*pid*-x *enp* plants were always sterile. *A second set of plants/flowers analysed. **Two stems carried terminal flowers.

The role of *ENP* in sepal and gynoecia development is also evident in plants with the genotype *pid-15 enp*/+ *enp*. These plants exhibit a conspicuous floral phenotype. Sepals are regularly fused to form a 'sepal ring', which ties up the other flower organs, causing reduced fertility by separating stamens from stigmata (Fig. 4). We noticed that *pid-15 enp*/*pid-15* + plants have apparently fewer flowers than *pid-15* +/*pid-15* + plants and those (abnormal) flowers are either infertile or have difficulties in producing *laterne* seeds (see Table S1 in the supplementary material).

The position of PIN1 in epidermal cells of the *laterne* embryo apex is reversed

ENP could act on PINOID in a variety of different ways. We tested two hypotheses: first, that it may affect on transcription; and second, that it may affect on auxin transport. RT-PCR analysis revealed that *pid* transcripts are still present in *laterne* seedlings (see Fig. S2 in the supplementary material) showing that *ENP* does not regulate *PID* transcription.

We tested net auxin flux as well as the polarity of auxin transport in both *pid* and *laterne* mutants. Auxin transport is not completely abolished in stems of *pinoid* plants (Bennet et al., 1995). Both *pinoid* and *laterne* showed a significant reduction in comparison with the wild type (Materials and methods; see Table S4 in the supplementary material). However, a significant difference in polar ^{14}C-IAA transport between *pinoid* and *laterne* was not observed. Thus, *enp*, in *pid* homozygous background, does not further reduce auxin transport in stems.

We then assessed the polarity of auxin transport by analysing the cellular position of PIN1 in the epidermis at the apex of wild-type, *pid* and *laterne* embryos. Laser-scanning microscopy was carried out predominantly on embryos at mid heart and torpedo stages, as clear polar PIN1-position was difficult to discern in globular to early heart stages, in both mutant and wild-type embryos (Fig. 6). All *laterne* embryos analysed (n>50) showed a striking reversal of polar PIN1 position when compared with wild-type (n>80) and *pid* embryos (n>50). Generally, three or four cell rows of the apex of *laterne* embryos carry detectable amounts of PIN1:GFP in the plasma membrane. Owing to the intense signalling, we cannot exclude PIN1 localisation on the apical side of cells in the upper rows. However, the predominant or exclusive position is clearly at the lateral and basal sides of the cells in *laterne*, where it is particularly well seen in the most basal cell rows (Fig. 6A-C). Pronounced lateral positioning of PIN1 is also found in the SAM region and increasingly towards the tips of cotyledon primordia in wild-type (Fig. 6D-F) and *pid* embryos (Fig. 6G,H). However, at the basal and mid region of wild-type cotyledon primordia, PIN1 is clearly localised at the apical side of the cells (Fig. 6D-F) (Steinmann et al., 1999; Benkova et al., 2003). Interestingly, although PIN1 changes its cellular position from apical to basal in apices of adult *pinoid* mutants (Friml et al., 2004), the situation is more complicated in cotyledon primordia of *pid-15* homozygous embryos. We detected apical positioning as seen in wild-type but frequently, even within the same primodia, we saw cells with basal localisation (Fig. 6G,H).

Auxin maxima are altered in *laterne* and *pinoid* embryos

The *DR5rev::GFP* construct described in Friml et al. (Friml et al., 2003) was used to examine auxin maxima in *laterne*, *pinoid* and wild-type embryos. Young wild-type heart stage embryos (n=70) always exhibit root maxima but mostly no clear cotyledon maxima (Fig. 7A; sometimes only weak ones), whereas torpedo embryos regularly showed well developed maxima (Fig. 7B,C). In addition to those mentioned, we found a weak wild-type maximum that develops in the incipient shoot apical meristem region during the torpedo stage (Fig. 7B,I). The *laterne* embryos always display the expected root meristem maximum but they do not

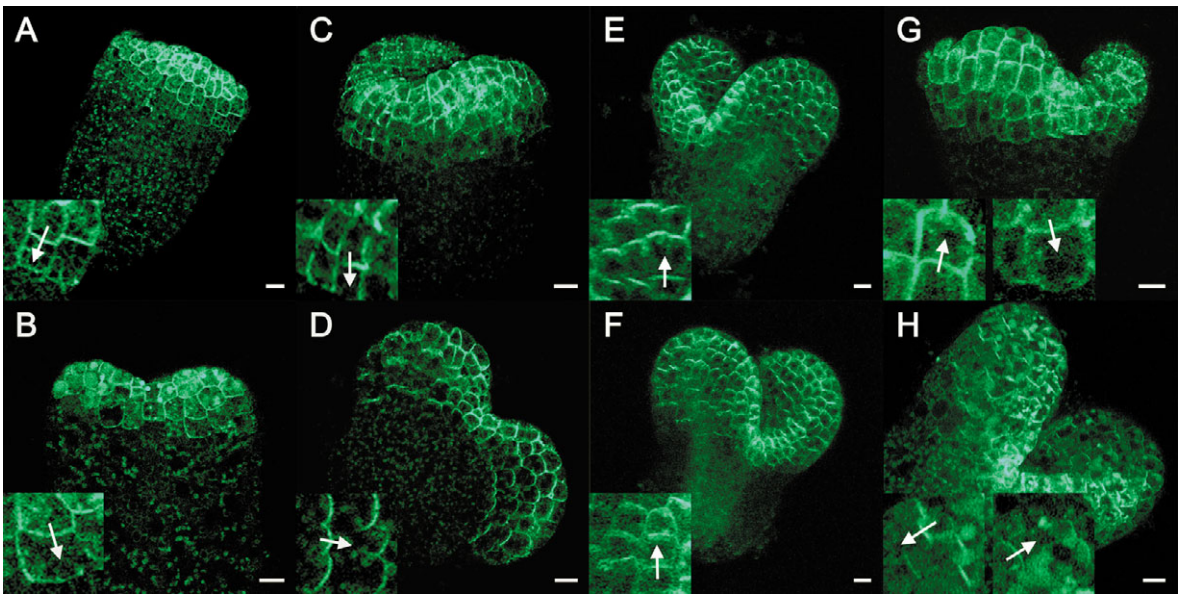

Fig. 6. PIN1:GFP localisation in *laterne (pid-15 enp)*, wild-type and *pid-15* embryos. (A-C) *laterne*, (D-F) wild type (G,H) and *pinoid* (all embryos between early and mid heart stage). Insets show higher magnifications; white arrows indicate PIN1:GFP cellular localisation. which is basal in A-C,G (right inset) and H (left inset), and apical in D-F,G (left inset) and H (right inset). Scale bars: 10 μm.

show any at the hypocotyl/epicotyl borders where cotyledons are expected to occur. Instead, they often display (split) SAM maxima that spread along the entire apical pole (Fig. 7K,L) or, conversely, are very weak (Fig. 7M). A further intriguing effect was detected when plants were analysed that either segregate both *pid* and *enp*, or *pid* alone (Fig. 7D-H). In these lines, *pid* embryos with three or two cotyledons occur, which exhibit disturbances with respect to their cotyledon but not to their root maxima. In some embryos, all cotyledon maxima were missing (Fig. 7F,G), in others, only one was missing and/or the other(s) displayed a discontinuous pattern (Fig. 7D,E,H).

Expression domains of meristem and organ specific genes in *laterne* embryos

The first morphological manifestation of the *pid enp* double mutation becomes visible at the early heart stage (compare Fig. 3 with Figs 8, 9). We carried out in situ hybridisation analyses with genes controlling the organisation of the embryo apex. Obvious alterations of gene expression were only observed in embryos that could be identified as *laterne* by their morphology (i.e. from triangular/early heart stage onwards). The analyses did not reveal conspicuous deviations of gene expression from wild-type for + *enp*/+ *enp* embryos.

In globular stage embryos, the transcription of *STM* displays a median stripe-like pattern indicating the anlagen of future shoot apical meristem (Fig. 8A,B). Later on *STM* is restricted to the central domain of this region (Fig. 8D,G). Alterations become visible in *laterne* from the triangular or early heart stage onwards (Fig. 8C,E), such that *STM* expands along the whole apical region (Fig. 8F,H). Interestingly, radial sections of this domain show that different embryos display a variability of expression, such that smaller regions with stronger and other with weaker signal strength appear (Fig. 8C,F,H).

The gene *ANT* is initially expressed in the circumference of the apical pole in a ring-like pattern (Fig. 8I). Its expression then concentrates at the sites of cotyledon initiation and is always found at young leaf primordia tips (Fig. 8K). During further development *ANT* transcripts accumulate at the precursor cells of xylem/phloem elements (Fig. 8M,O). In *laterne*, *ANT* extends along the apical pole with a variable localisation (Fig. 8N,P) but remains absent in the centre (Fig. 8L,N,P), explaining why *laterne* does not generate leaves in this sector.

CUC2 expression overlaps with *STM* in the globular embryo and forms later a 'ring' separating shoot meristem and cotyledons (Fig. 8Q,R,T,U,W). Similar to *ANT*, the *CUC2* localisation embraces the whole apical pole with patch-like patterns (Fig. 8V). In addition, it is sometimes also found in the centre (Fig. 8S,V,X). In wild-type as well as *laterne*, the expression patterns of *ANT* and *CUC2* are partly overlapping in early stages and then separate in later stages. Expression of *ANT*, *CUC2* and *STM* in tricotyledoneous *pid-15* +/*pid-15* + embryos, as well as the topology of the apical pole (not shown), was comparable with that in wild type (see Fig. S3 in the supplementary material; the domain of *STM* was slightly enlarged). Two *GUS* constructs suggest that other genes organising the topmost meristem region, such as *KNAT2* and *CUC3,* exhibit similar alterations (see Fig. S4 in the supplementary material).

In wild-type the *WUS* domain initially embraces the internal (non-epidermal) cells in the upper half of the 16-cell stage. With progressing development, *WUS* is restricted to a few cells in L3 immediately neighboured to the vascular precursor cells of the central cylinder (Fig. 9A-C,E,G). We reasoned that in *laterne*, this cell group is localised in a region that morphologically displays wild-type organisation. In fact, in situ analysis shows that *WUS* expression is almost the same in *laterne* and wild-type embryos (Fig. 9).

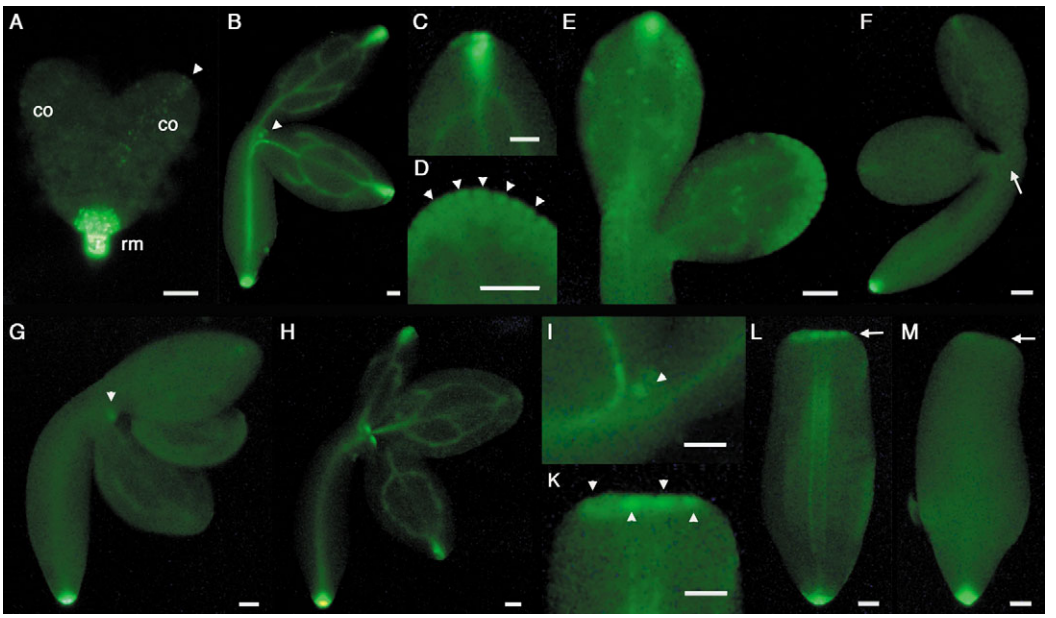

Fig. 7. Auxin maxima in wild-type, *pid-15* and *laterne* (*pid-15 enp*) embryos. (A-C,I) Wild-type embryos; (D-H) *pinoid* embryos; (K-M) *laterne* embryos. (A) Heart stage (arrowhead points to weak signal); (B,E-H,L,M) mid torpedo stage; (C) detail of B; (D) detail of E; (I) detail of B (reversed picture); (K) detail of L. Arrowheads indicate maxima. The arrow indicates the missing shoot maximum in F and a variable shoot maximum in L and M. co, cotyledon; rm, root meristem precursor. Scale bars: 20 μm.

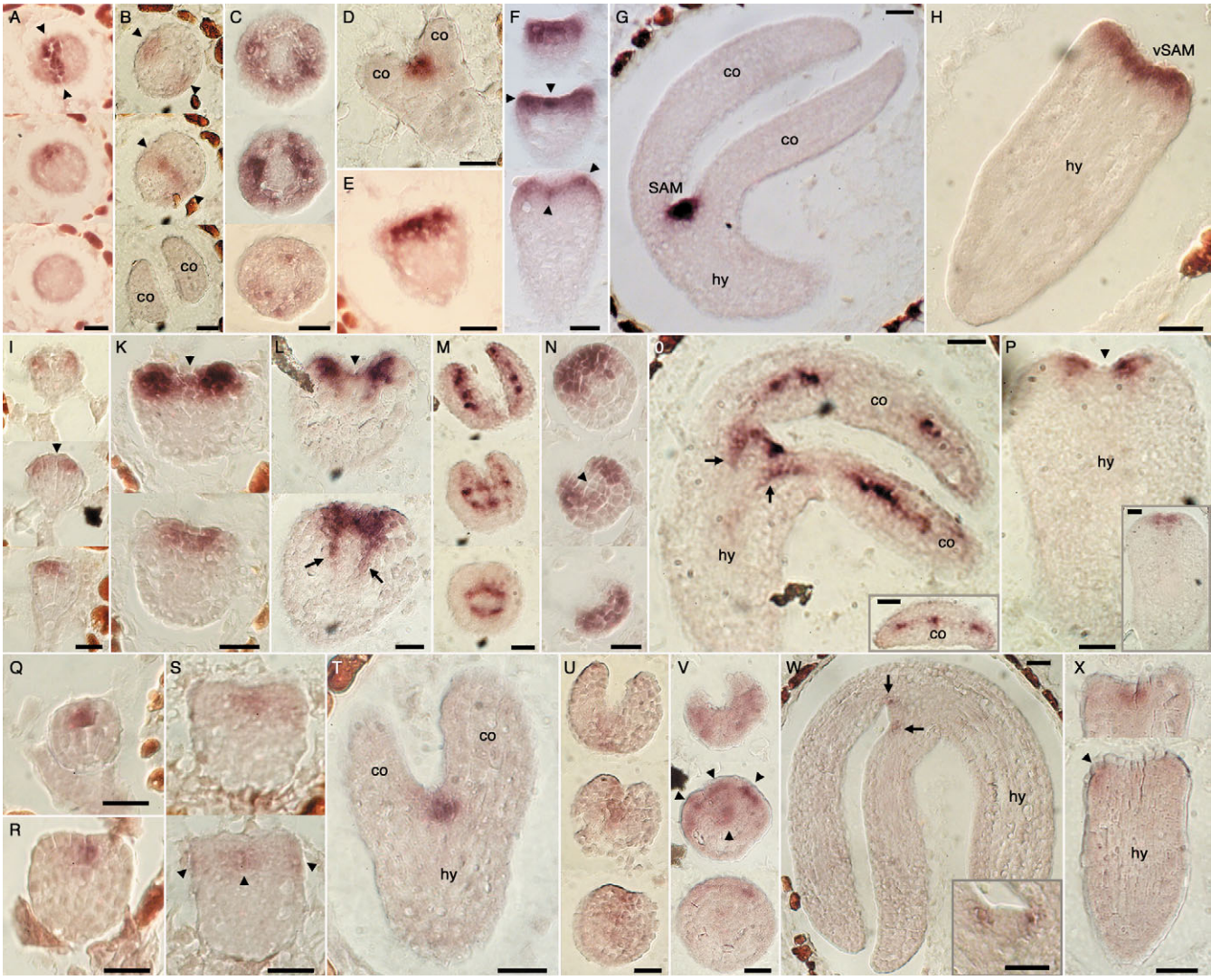

Fig. 8. Expression of *STM*, *ANT* and *CUC2* in wild-type and *laterne* (*pid-15 enp*) embryos. (A,B,D,G,I,K,M,O,Q,R,T,U,W) Wild-type, (C,E,F,H,L,N,P,S,V,X) *laterne*, (A-H) *STM* expression, (I-P) *ANT* expression and (Q-X) *CUC2* expression. (A-C,F,I-N,S,U,V,X) Arranged in series (top to bottom). (A,B) Cross-section series (top view) of globular stage (A) and heart stage embryo (B) with stripe-like domain of *STM* expression (arrowheads). (C) Cross section heart stage (top view). (D,E) Lateral views of wild-type (D) and *laterne* (E) heart stage embryos. (F) Tangential to median sections of young *laterne* torpedo stage (black arrowheads indicate patches of higher intensity). (G) Wild-type torpedo with *STM* expression defining the SAM. (H) Comparable picture of *laterne* torpedo, with patch-like pattern of *STM* signal. (I,K) Longitudinal series showing the ring-like *ANT* expression pattern in globular stage (I) and stained cotyledon primordia in heart stage (K). The black arrowheads in I and K indicate the central region lacking ANT. (L) Longitudinal series of *laterne* heart stage with *ANT* expression (arrowhead indicates emerging apical cavity without signal; arrows indicate emerging expression in vascular precursors). (M) Wild-type cross-section series with signal concentration in vascular precursors. (N) Cross-section series shows extension of *ANT* domain in apical pole of *laterne*, avoiding the centre (arrowhead). (O) Longitudinal section of wild-type torpedo (slightly out of centre; arrows as in L). Inset shows cotyledon cross-section. (P) Longitudinal section of *laterne* torpedo (arrowhead: apical cavity lacks *ANT* signal). Inset displays tangential cut to stress ring-shaped *ANT* expression. (Q,R) Globular (Q) and early heart stage (R) each with *CUC2* expression. (S) *laterne* heart stage longitudinal series with distributed patches of expression (arrowheads). (T) Wild-type at late heart stage. (U) Wild-type cross-section series indicating the early stripe-like pattern. (V) A *laterne* cross-section (arrowheads: expression peaks); signal is also present in the centre. (W) Longitudinal section in torpedo embryo with lateral (ring-shaped) signals, avoiding the central SAM region (arrows). The inset is at a higher magnification. (X) Series of torpedo stage *laterne* with distributed expression (arrowhead). co, cotyledon; hy, hypocotyl; SAM, shoot apical meristem; vSAM, variable SAM. Scale bars: 20 μm.

The seedling phenotypes of *laterne* and *pid-15 enp stm-5* homozygous mutants are identical

Furutani et al. (Furutani et al., 2004) showed that *pin1 pid* double mutants, in part, do not develop cotyledons and that cotyledon formation could be restored when meristem specifying functions were abolished by introducing mutations in *STM* or *CUC* genes. With this in mind, we tested the effect of adding *stm-5* (a strong allele) to the double mutant *pid-15 enp* (see Materials and methods). In fact, 12/62 *laterne* progeny of this cross were homozygous *pid-15 enp stm-5* (Fig. 10A).

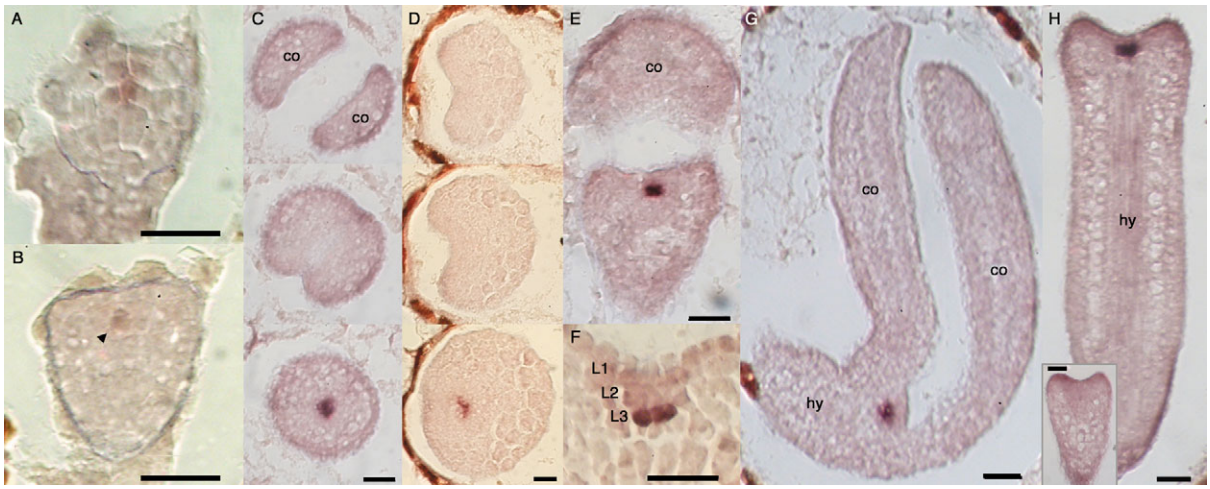

Fig. 9. *WUS* expression in wild-type and *laterne* (*pid*-15 *enp*/*pid*-15 *enp*) embryos. (A-C,E,G) Wild-type, (D,F,H) *laterne*. (A) *WUS* expression is found in L2 and L3 in wild-type globular stage. (B) Signal restricts to L3 in early heart stage (arrowhead). (C,D) Cross-section series of wild-type heart stage (C) and *laterne* torpedo stage (D), both with wild-type signal location. (E) Median section of the wild-type shows shoot apical pole and only part of one cotyledon (co) with *WUS* signal in L3. (F) Higher magnification of comparable *laterne* region exhibiting the same location in L3 (tissue layers L1-L3 indicated). (G,H) Longitudinal section of late torpedo stage wild-type (G) and *laterne* (H) with *WUS* signal. The inset (H) shows sense hybridisation. co, cotyledon; hy, hypocotyl. Scale bars: 20 μm.

Other *laterne* individuals were either *pid-15 enp +/pid-15 enp stm-5* or homozygous *pid-15 enp* + (Fig. 10B). Note that the seedling phenotype of homozygous *pid-15* + *stm-5* was rather additive (see Materials and methods). This demonstrates that restoration of cotyledon formation is not possible in *laterne* by eliminating the meristem specifying function of *STM*. By contrast, the *stm-5* mutation can be partly overcome in the triple mutant as regards the production of true leaves (Fig. 10A,B,D). In addition, adult stages of double and triple mutants were comparable (not shown).

Discussion

Mutations in *ENHANCER OF PINOID* and *PINOID* cause the *laterne* phenotype

The double mutant combination of a hitherto unknown locus, *enhancer of pinoid*, and *pinoid* causes failure of cotyledon primordia and thus a precise deletion of cotyledons in embryogenesis, which gives rise to *laterne* seedlings. In contrast to other known mutations that affect the cotyledons, or combinations thereof, the embryonic hypocotyl and root are unaffected. As *enp* plants have only a subtle post-embryonic phenotype, we conclude that *ENP* acts as a specific modifier of *PINOID* and that together these two loci instruct precursor cells to elaborate cotyledons in the transition stage embryo.

The SAM in *laterne* mutants is enlarged and indented. Possibly, the presence of cotyledons is required during embryogenesis to define and organise the SAM properly (Torres Ruiz, 2004). This would be reminiscent of postembryonic development where genes expressed in the adaxial and abaxial sides of leaves are thought to influence SAM development (Siegfried et al., 1999; Sawa et al., 1999; McConnell et al., 2001; Kerstetter et al., 2001; Kumaran et al., 2002; Tsukaya, 2002). Double mutant combinations of *cuc1*, *cuc2* and *cuc3* genes, which develop one fused cotyledon and no SAM, suggested a requirement of bilateral symmetry and cotyledon boundaries for SAM formation (Aida et al., 1997; Aida et al., 1999; Vroemen et al., 2003). However, deletion of cotyledons causes loss of bilateral symmetry in *laterne* but is not a prerequisite for SAM formation.

Dose effects indicate tight genetic interaction between *ENHANCER OF PINOID* and *PINOID*

The synergistic effect of the *pid* and *enp* mutations are indicative of a genetic interaction during early embryogenesis. We detected dose-dependent effects, which suggest an additional tight interaction at late adult development. The homozygous *enp* adult phenotype is very subtle, yet with addition of a single *pid* mutant allele

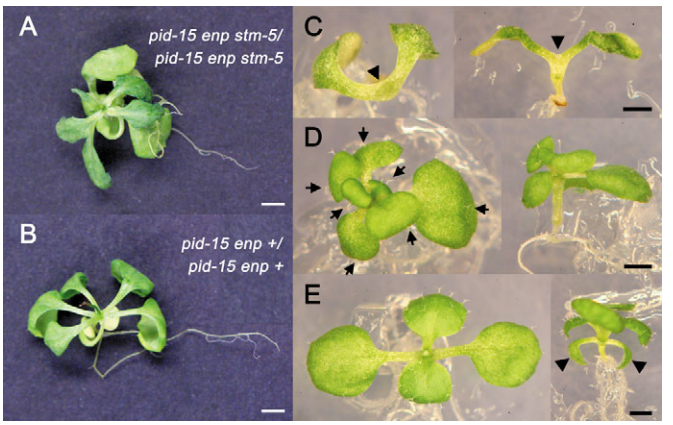

Fig. 10. Analysis of triple mutant *pid-15 enp stm-5*. (A,B) Seedling phenotype of triple (A) versus double (B) mutant (genotypes indicated). (C-E) Comparison of *stm-5* (C), *laterne* (D) and wild-type (E) phenotype. Arrowheads and arrows respectively indicate shoot meristemless region between the cotyledons (C), trichomes of adult leaves (D) and trichomless cotyledons (E). Scale bars: 2.5 mm in A,B; 1 mm in C-E.

the frequency and expressivity of this phenotype, i.e. fused sepals, is greatly enhanced. Similarly, a single *enp* mutant allele has an effect on the fertility of *pid* mutants. Such dose effects might, for example, be due to physical interaction of the participating gene products. However, *ENP* (as inferred from its position) has not been detected as an interactor of PID, in yeast-two-hybrid screens (Benjamins et al., 2003). Therefore, further work will be necessary to clarify the mode of interaction between these two genes.

STM domain expansion in *laterne* does not cause cotyledon failure, indicating the essential role of *ENP* for cotyledon development

In wild type, *STM* and *CUC2* domains initially overlap in the central region of the embryo apex and are then refined, such that *STM* remains in the centre while *CUC2* shifts to the cotyledon boundary regions (Long et al., 1996; Long and Barton, 1998; Aida et al., 1997; Aida et al., 1999). *ANT* is expressed in a ring-shaped pattern at the globular stage, in cotyledon primordia at the heart stage and in the vascular precursor cells as of the torpedo stage (Elliott et al., 1996; Klucher et al., 1996). In *laterne STM*, *KNAT2, ANT, CUC2* and *CUC3* expand along the entire upper pole, initially in an uniform manner but later (at the torpedo stage) in a punctate and mostly overlapping fashion. This correlates well with the variability in post-embryonic leaf production. By contrast, expression of *WUS*, the gene that induces stem cell identity (Mayer et al., 1998; Schoof et al., 2000; Brand et al., 2000), remains perfectly wild-type, despite *WUS*-expressing cells are immediately adjacent to the abnormal epicotyl. Other factors, such as the inductive capability of the adjacent vascular precursor cells (Jürgens, 2001), seem to control *WUS* and thus the determination of stem cells.

STM activity in wild-type embryos functions to maintain SAM cells in an undifferentiated state. The expanded *STM* domain in *laterne* mutants might likewise act to maintain cells that would normally give rise to cotyledons in an undifferentiated state. A comparable observation has been made in *pin1 pid* double mutants, which frequently lack cotyledons. Interestingly cotyledon development is partially recovered in *pin1 pid stm* (Furutani et al., 2004), suggesting that a basic developmental machinery for cotyledon development was suppressed in the double mutant. Similarly, in post-embryonic development, simultaneous elimination of the competing activities of *STM* and *AS1* leads to (partial) meristem recovery (Byrne et al., 2000). The triple mutant *pid enp stm* revealed that loss of *STM* function can be (partly) overcome to produce rosette leaves on top of the apex. Note, however, that in *stm* mutants, leaves occasionally emerge from the hypocotyl (Barton and Poethig, 1993). More importantly, the *pid enp stm* homozygous mutant displays a *laterne* seedling phenotype. Thus action of *ENP* cannot be bypassed, as shown in the *STM PID PIN1* 'pathway', to rescue the generation of cotyledons. Rather, this analysis suggests that PIN1, PID and ultimately ENP partly control *STM* expression. The molecular mechanism remains unclear but recently it has been reported that, for example, PIN genes restrict expression of *PLETHORA* genes, major determinants of root stem cell specification (Blilou et al., 2005).

ENP appears to exert its effect by specifically reverting the polarity of auxin transport in the *pinoid* background

The Ser/Thr kinase *PINOID* has recently been shown to control polar targeting of the PIN1 auxin transport facilitator in plasma membranes of epidermal cells of the inflorescence meristem. Loss-of-function *pid* mutations result in basal, rather than apical, targeting of PIN1 (Friml et al., 2004). This reverses auxin transport away from presumptive organ primordia and abolishes the accumulation of auxin maxima, the reference points for organ formation (Benkova et al., 2003; Reinhardt et al., 2000; Reinhardt et al., 2003). Consequently, *pinoid* mutants display abnormal or missing (floral) organs and disturbed phyllotaxis (Bennett et al., 1995; Christensen et al., 2000; Benjamins et al., 2001; Friml et al., 2003; Reinhardt et al., 2003).

In line with observations regarding the importance of auxin for cotyledon formation (e.g. Hadfi et al., 1998), mutations in *PID* as well as in *PIN1* cause abnormal cotyledon numbers. Notably, these mutants do lead to cotyledon abnormalities but not to loss of cotyledons (with rare exceptions). One possibility to explain this is that redundant homologs mask cotyledon effects of the single mutants. For example, root development is guided by the combined action of several PIN genes; single mutants have relatively mild effects (Friml et al., 2003; Blilou et al., 2005). Similarly, as *PID* belongs to a gene family with 23 members in *Arabidopsis* (Friml et al., 2004), multiple PID genes could control cotyledon development. By virtue of position and preliminary sequence data (we sequenced a *PID*-like candidate gene residing in the mapped region), *ENP* is not a *PID* (nor a PIN) homolog. However, if other members of these families are recruited for cotyledon development, *ENP* could possibly enhance more than one gene. Cloning of *ENP* and molecular screening for interactors will clarify this question.

Although the impact of redundant genes on cotyledon development can still not be excluded, analysis of PIN1 polarity very probably revealed how *enp* enhances *pid*. Interestingly, and in contrast to adult *pinoid* plants, *pid* embryos exhibit frequent but not complete reversal of PIN1 positioning in the epidermis of the embryo apex. According to the proposed models for organ formation (Benkova et al., 2003), auxin flux should be partly reversed but the net flux in

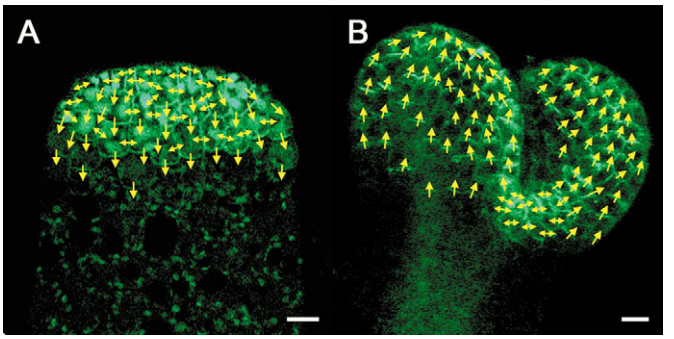

Fig. 11. Auxin flux in the epidermis of the *laterne* apex. Arrows indicate direction of auxin transport as deduced from PIN1:GFP cellular position. (A) Apex of a *laterne* (*pid-15 enp*) embryo. (B) Apex of a wild-type embryo. Scale bars: 10 μm.

the *pid* apex is still directed towards the cotyledon tip. This disturbance is apparently strong enough to cause mild cotyledon defects including an aberrant cotyledon phyllotaxis. However, regarding the generation of cotyledons per se, either auxin maxima are not required for organogenesis or auxin plays a role in cotyledon development, at concentrations not sufficient to induce visible *DR5rev::GFP* signals. The latter is supported by wild-type heart stage embryos, which in our analysis only occasionally displayed weak auxin maxima. This situation is reminiscent of the double root phenotypes of *topless,* which only exhibit the root tip auxin maximum, required for correct root pattern (Sabatini et al., 1999; Friml et al., 2003), in the 'normal' basal root but not in the apical root (Long et al., 2002).

Analysis of *laterne* embryos unambiguously shows that apical localisation of PIN1 in the epidermis is completely reversed to basal, i.e. *enp* enhances the mild defect observed in *pid*. In addition, marked lateral positioning as found in cells of the SAM region in wild type, is seen. We postulate that this is why cotyledons are not formed in *laterne*. Auxin coming from basal cells would be 'repulsed' by these apical cells, whereas any auxin synthesized in the apex would circulate around the apex and be ultimately transported downwards (Fig. 11). In the vascular precursor cells, PIN1 is positioned at the basal cell pole regardless of whether the embryo is mutant or not. Consequently, in *laterne*, the presumptive cotyledon anlage retain little or no auxin and organ initiation is not possible.

We thank Christine Stockum, Miriam Vogg, Florian Brückner, Michael Schurig and Andrea Lohner for valuable help and technical assistance; Gerd Jürgens, Kay Schneitz, Lynette Fulton and, especially, Farhah Assaad for critical regard of the manuscript; and Monika Frey for useful discussions. We thank the Nottingham *Arabidopsis* Stock Center and the following colleagues for lines and clones: Casper Vroemen, Kathy Barton, David Smyth, Jan Dox, Jiri Friml, Masao Tasaka, Mitsuhiro Aida, Sacco de Vries, Sioux Christensen and Thomas Laux. We owe special thanks to Yehuda Ben Shaul (University of Tel Aviv) for scanning electron microscopy pictures. We are particularly indepted to Alfons Gierl for his consistent and generous support throughout all phases of this and other projects.

Supplementary material

Supplementary material for this article is available at
http://dev.biologists.org/cgi/content/full/132/18/4063/DC1

References

Aida, M., Ishida, T., Fukaki, H., Fujisawa, H. and Tasaka, M. (1997). Genes involved in organ separation in *Arabidopsis*: an analysis of the *cup-shaped cotyledon* mutant. *Plant Cell* **9**, 841-857.

Aida, M., Ishida, T. and Tasaka, M. (1999). Shoot apical meristem and cotyledon formation during *Arabidopsis* embryogenesis: interaction among the *CUP-SHAPED COTYLEDON* and *SHOOT MERISTEMLESS* genes. *Development* **126**, 1563-1570.

Barton, M. K. and Poethig, R. S. (1993). Formation of the shoot apical meristem in *Arabidopsis thaliana*: an anlysis of development in the wild-type and in the shoot meristemless mutant. *Development* **119**, 823-831.

Baud, S., Bellec, Y., Miquel, M., Bellini, C., Caboche, M., Lepiniec, L., Faure, J. D. and Rochat, C. (2004). *gurke* and *pasticcino3* mutants affected in embryo development are impaired in acetyl-CoA carboxylase. *EMBO J.* **5**, 515-520.

Benjamins, R., Quint, A., Weijers, D., Hooykaas, P. and Offringa, R. (2001). The PINOID protein kinase regulates organ development in *Arabidopsis* by enhancing polar auxin transport. *Development* **128**, 4057-4067.

Benjamins, R., Ampudia, C. S., Hooykaas, P. J. and Offringa, R. (2003). PINOID-mediated signaling involves calcium-binding proteins. *Plant Physiol.* **132**, 1623-1630.

Benkova, E., Michniewicz, M., Sauer, M., Teichmann, T., Seifertova, D., Jurgens, G. and Friml, J. (2003). Local, efflux-dependent auxin gradients as a common module for plant organ formation. *Cell* **115**, 591-602.

Bennett, S. R. M., Alvarez, J., Bossinger, G. and Smyth, D. R. (1995). Morphogenesis in *pinoid* mutants of *Arabidopsis thaliana. Plant J.* **8**, 505-520.

Berleth, T. and Jürgens, G. (1993). The role of the *monopteros* gene in organising the basal body region of the *Arabidopsis* embryo. *Development* **118**, 575-587.

Berleth, T. and Chatfield, S. (2002). Embryogenesis: Pattern Formation from a Single Cell. In *The* Arabidopsis *Book* (ed. C. R. Somerville and E. M. Meyerowitz). Rockville, MD: American Society of Plant Biologists. doi/10.1199/tab.0051

Blilou. I., Xu, J., Wildwater, M., Willemsen, V., Paponov, I., Friml, J., Heidstra, R., Aida, M., Palme, K. and Scheres, B. (2005). The PIN auxin efflux facilitator network controls growth and patterning in *Arabidopsis* roots. *Nature* **433**, 39-44.

Brand, U., Fletcher, J. C., Hobe, M., Meyerowitz, E. M. and Simon, R. (2000). Dependence of the stem cell fate in *Arabidopsis* on a feedback loop regulated by CLV3 activity. *Science* **289**, 817-819.

Byrne, M. E., Barley, R., Curtis, M., Arroyo, J. M., Dunham, M., Hudson, A. and Martienssen, R. A. (2000). *Asymmetric leaves1* mediates leaf patterning and stem cell function in *Arabidopsis*. *Nature* **408**, 967-971.

Christensen, S. K., Dagenais, N., Chory, J. and Weigel, D. (2000). Regulation of auxin response by the protein kinase *PINOID*. *Cell* **100**, 469-478.

Conway, L. J. and Poethig, R. S. (1997). Mutations of *Arabidopsis thaliana* that transform leaves into cotyledons. *Proc. Natl. Acad. Sci. USA* **94**, 10209-10214.

Elliott, R. C., Betzner, A. S., Huttner, E., Oakes, M. P., Tucker, W. Q., Gerentes, D., Perez, P. and Smyth, D. R. (1996). *AINTEGUMENTA*, an *APETALA-2* like gene in *Arabidopsis* with pleiotropic roles in ovule development and floral organ growth. *Plant Cell* **8**, 155-168.

Erschadi, S., Haberer, G., Schöniger, M. and Torres Ruiz, R. A. (2000). Estimating genetic diversity of *Arabidopsis thaliana* ecotypes with Amplified Fragment Length Polymorphisms (AFLP). *Theor. Appl. Genet.* **100**, 633-640.

Friml, J., Vieten, A., Sauer, M., Weijers, D., Schwarz, H., Hamann, T., Offringa, R. and Jurgens, G. (2003). Efflux-dependent auxin gradients establish the apical-basal axis of *Arabidopsis*. *Nature* **426**, 147-153.

Friml, J., Yang, X., Michniewicz, M., Weijers Quint, A., Tietz, O., Benjamins, R., Ouwerkerk, P. B. F., Ljung, K., Sandberg, G., Hooykaas, P. J. J. et al. (2004). A *PINOID*-dependent binary switch in apical-basal PIN polar targeting directs auxin efflux. *Science* **306**, 862-865.

Furutani, M., Vernoux, T., Traas, J., Kato, T., Tasaka, M. and Aida, M. (2004). *PIN-FORMED1* and *PINOID* regulate boundary formation and cotyledon development in *Arabidopsis* embryogenesis. *Development* **131**, 5021-5030.

Gälweiler, L., Guan, C., Müller, A., Wisman, E., Mendgen, K., Yephremov, A. and Palme, K. (1998). Regulation of polar auxin transport by AtPIN1 in *Arabidopsis* vascular tissue. *Science* **282**, 2226-2230.

Geldner, N., Richter, S., Vieten, A., Marquardt, S., Torres-Ruiz, R. A., Mayer, U. and Jürgens, G. (2004). Partial loss-of-function alleles reveal a role for GNOM in post-embryonic and auxin-transport related development of *Arabidopsis*. *Development* **131**, 389-400.

Haberer, G., Erschadi, S. and Torres Ruiz, R. A. (2002). The *Arabidopsis* gene *PEPINO/PASTICINO2* is required for proliferation control of meristematic and non-meristematic cells and encodes a putative anti-phosphatatse. *Dev. Genes Evol.* **212**, 542-550.

Hadfi, K., Speth, V. and Neuhaus, G. (1998). Auxin-induced developmental patterns in *Brassica juncea* embryos. *Development* **125**, 879-887.

Iwakawa, H., Ueno, Y., Semiarti, E., Onouchi, H., Kojima, S., Tsukaya, H., Hasebe, M., Soma, T., Ikezaki, M., Machida, C. and Machida, Y. (2002). The *ASYMMETRIC LEAVES2* gene of *Arabidopsis thaliana*, required for formation of a symmetric flat leaf lamina, encodes a member of a novel family of proteins characterized by cysteine repeats and a leucine zipper. *Plant Cell Physiol.* **5**, 467-478.

Jürgens, G. (2001). Apical-basal pattern formation in *Arabidopsis* embryogenesis. *EMBO J.* **20**, 3609-3616.

Kaplan, D. (1969). Seed development in Downingia. *Phytomorphology* **19**, 253-278.

Kaplan, D. R. and Cooke, T. J. (1997). Fundamental concepts in the embryogenesis of dicotyledons – a morphological interpretation of embryo mutants. *Plant Cell* **9**, 1903-1919.

Kerstetter, R. A., Bollman, K., Taylor, R. A., Bomblies, K. and Poethig, R. S. (2001). *KANADI* regulates organ polarity in *Arabidopsis. Nature* **411**, 706-709.

Klucher, K. M., Chow, H., Reiser, L. and Fischer, R. L. (1996). The *AINTEGUMENTA* gene of *Arabidopsis* required for ovule and female gametophyte development is related to the floral homeotic gene *APETALA2*. *Plant Cell* **8**, 137-153.

Kumaran, M. K., Bowman, J. L. and Sundaresan, V. (2002). *YABBY* polarity genes mediate the repression of *KNOX* homeobox genes in *Arabidopsis. Plant Cell* **14**, 2761-2770.

Ljung, K., Bhalerao, R. P. and Sandberg, G. (2001). Sites and homeostatic control of auxin biosynthesis in *Arabidopsis* during vegetative growth. *Plant J.* **28**, 465-474.

Long, J. A. and Barton, M. K. (1998). The development of apical embryonic pattern in *Arabidopsis*. *Development* **125**, 3027-3035.

Long, J. A., Moan, E. I., Medford, J. I. and Barton, M. K. (1996). A member of the *KNOTTED* class of homeodomain proteins encoded by the *STM* gene of *Arabidopsis*. *Nature* **379**, 66-69.

Long, J. A., Woody, S., Poethig, S., Meyerowitz, E. M. and Barton, M. K. (2002). Transformation of shoots into roots in *Arabidopsis* embryos mutant at the *TOPLESS* locus. *Development* **129**, 2297-2306.

Lotan, T., Ohto, M., Yee, K. M., West, M. A. L., Lo, R., Kwong, R., Yamagishi, K., Fischer, R. L., Goldberg, R. B. and Harada, J. J. (1998). *Arabidopsis LEAFY COTYLEDON1* is sufficient to induce embryo development in vegetative cells. *Cell* **93**, 1195-1205.

Lukowitz, W., Gillmor, C. S. and Scheible, W. R. (2000). Positional cloning in *Arabidopsis.* Why it feels good to have a genome initiative working for you. *Plant Physiol.* **123**, 795-805.

Lynn, K., Fernandez, A., Aida, M., Sedbrook, J., Tasaka, M., Masson, P. and Barton, M. K. (1999). The *PINHEAD/ZWILLE* gene acts pleiotropically in *Arabidopsis* development and has overlapping functions with the *ARGONAUTE* gene. *Development* **126**, 469-481.

Mayer, K. F. X., Schoof, H., Haecker, A., Lenhard, M., Jürgens, G. and Laux, T. (1998). Role of *WUSCHEL* in regulating stem cell fate in the *Arabidopsis* shoot meristem. *Cell* **95**, 805-815.

Mayer, U., Torres Ruiz, R. A., Berleth, T., Misera, S. and Jürgens, G. (1991). Mutations affecting body organization in the *Arabidopsis* embryo. *Nature* **353**, 402-407.

Mayer, U., Büttner, G. and Jürgens, G. (1993). Apical-basal pattern formation in the *Arabidopsis* embryo: studies on the role of the *GNOM* gene. *Development* **117**, 149-162.

McConnell, J. R., Emery, J., Eshed, Y., Bao, N., Bowman, J. and Barton, M. K. (2001). Role of *PHABULOSA* and *PHAVOLUTA* in determining radial patterning in shoots. *Nature* **411**, 709-713.

Meinke, D. W. (1992). A homeotic mutant of *Arabidopsis thaliana* with leafy cotyledons. *Science* **258**, 1647-1650.

Moussian, B., Schoof, H., Haecker, A., Jürgens, G. and Laux, T. (1998). Role of the *ZWILLE* gene in the regulation of central shoot meristem cell fate during *Arabidopsis* embryogenesis. *EMBO J.* **17**, 1799-1809.

Okada, K., Ueda, J., Komaki, M. K., Bell, C. J. and Shimura, Y. (1991). Requirement of the auxin polar transport system in early stages of *Arabidopsis* floral bud formation. *Plant Cell* **3**, 677-684.

Reinhardt, D., Mandel, T. and Kuhlemeier, C. (2000). Auxin regulates the initiation and radial position of plant lateral organs. *Plant Cell* **12**, 507-518.

Reinhardt, D., Pesce, E. R., Stieger, P., Mandel, T., Baltensperger, K., Bennett, M., Traas, J., Friml, J. and Kuhlemeier, C. (2003). Regulation of phyllotaxis by polar auxin transport. *Nature* **426**, 255-260.

Sabatini, S., Beis, D., Wolkenfelt, H., Murfett, J., Guilfoyle, T., Malamy, J., Benfey, P., Leyser, O., Bechtold, N., Weisbeek, P. and Scheres, B. (1999). An auxin-dependent distal organizer of pattern and polarity in the *Arabidopsis* root. *Cell* **99**, 463-472.

Sawa, S., Watanabe, K., Goto, K., Kanaya, E., Morita, E. H. and Okada, K. (1999). *FILAMENTOUS FLOWER*, a meristem and organ identity gene of *Arabidopsis*, encodes a protein with a zinc finger and HMG-related domains. *Genes Dev.* **13**, 1079-1088.

Scheres, B., Di Laurenzio, L., Willemsen, V., Hauser, M.-T., Janmaat, K., Weisbeek, P. and Benfey, P. (1995). Mutations affecting the radial organisation of the *Arabidopsis* root display specific defects throughout the embryonic axis. *Development,* **121**, 53-62.

Schoof, H., Lenhard, M., Haecker, A., Mayer, K. F. X., Jürgens, G. and Laux, T. (2000). The stem cell population of *Arabidopsis* shoot meristems is maintained between a regulatory loop between the *CLAVATA* and *WUSCHEL* genes. *Cell* **100**, 635-644.

Siegfried, K. R., Eshed, Y., Baum, S. F., Otsuga, D., Drews, G. N. and Bowman, J. L. (1999). Members of the *YABBY* gene family specify abaxial cell fate in *Arabidopsis*. *Development* **126**, 4117-4128.

Steinmann, T., Geldner, N., Grebe, M., Mangold, S., Jackson, C. L., Paris, S., Gälweiler, L., Palme, K. and Jürgens, G. (1999). Coordinated polar localization of auxin efflux carrier PIN1 by GNOM ARF GEF. *Science* **286**, 316-318.

Stone, S. L., Kwong, L. W., Yee, K. M., Pelletier, J., Lepiniec, L., Fischer, R. L., Goldberg, R. B. and Harada, J. J. (2001). *LEAFY COTYLEDON2* encodes a B3 domain transcription factor that induces embryo development. *Proc. Natl. Acad. Sci. USA* **98**, 11806-11811.

Strasburger, E. (2002). *Lehrbuch der Botanik*, 35th edn. Berlin, Heidelberg: Spektrum Verlag.

Torres Ruiz, R. A. (2004). Polarity in Arabidopsis embryogenesis. In *Polarity in Plants* (ed. K. Lindsey), pp. 157-191. Oxford: Blackwell Publishers.

Torres Ruiz, R. A., Lohner, A. and Jürgens, G. (1996a). The *GURKE* gene is required for normal organization of the apical region in the *Arabidopsis* embryo. *Plant J.* **10**, 1005-1016.

Torres Ruiz, R. A., Fischer, T. and Haberer, G. (1996b). Genes involved in the elaboration of apical pattern and form in *Arabidopsis thaliana*: Genetic and molecular analysis. In *Embryogenesis: The Generation of a Plant.* (ed. E. Cummings and T. Wang), pp. 15-34. Oxford, UK: Bios Scientific Publishers.

Tsukaya, H. (2002). Leaf development. In *The* Arabidopsis *Book* (ed. C. R. Somerville and E. M. Meyerowitz). Rockville, MD: American Society of Plant Biologists. doi/10.1199/tab.0072

Vroemen, C. W., Mordhorst, A. P., Albrecht, C., Kwaaitaal, M. A. and de Vries, S. C. (2003). The *CUP-SHAPED COTYLEDON3* gene is required for boundary and shoot meristem formation in *Arabidopsis*. *Plant Cell* **15**, 1563-1577.